Tandem Pairing in Heavy-Fermion Superconductors

Rebecca Flint and Piers Coleman
Center for Materials Theory, Rutgers University, Piscataway, New Jersey 08854, USA
(Received 10 May 2010; published 8 December 2010)

We consider the internal structure of a d-wave heavy-fermion superconducting condensate, showing that it necessarily contains two components condensed in tandem: pairs of quasiparticles on neighboring sites and composite pairs consisting of two electrons bound to a single local moment. These two components draw upon the antiferromagnetic and Kondo interactions to cooperatively enhance the superconducting transition temperature. This tandem condensate is electrostatically active, with an electric quadrupole moment predicted to lead to a superconducting shift in the nuclear quadrupole resonance frequency.

DOI: 10.1103/PhysRevLett.105.246404 PACS numbers: 71.27.+a, 74.20.Mn, 74.25.Dw

In many strongly interacting materials, quasiparticles are ill formed at the superconducting transition, giving the Cooper pair a nontrivial internal structure. The 115 family of heavy-fermion superconductors [1–4] provides an extreme example of this phenomenon, where quasiparticle formation, through the screening of local moments by electrons, coincides with the onset of superconductivity.

The 115 family has long attracted great interest for the remarkable rise of the superconducting transition temperature from $T_c = 0.2$ K in $CeIn_3$ under pressure [5] to 2.3 K in $CeCoIn_5$ [1–3], rising to 18.5 K in $PuCoGa_5$ [4]. While the abundance of magnetism in the phase diagram has led to a consensus that spin fluctuations drive the superconductivity in the cerium compounds [5–9], the presence of unquenched local moments at T_c is difficult to explain within this picture. In a typical spin-fluctuation mediated heavy-fermion superconductor, the local moments quench to form a *Pauli paramagnet* [$\chi(T) \sim \chi_0$] well before the development of superconductivity. Yet $NpPd_5Al_2$ [10] and $Ce\{Co, Ir\}In_5$ [2,11] exhibit a Curie-Weiss susceptibility, $\chi(T) \sim 1/(T + T_{CW})$ down to T_c.

The absence of any magnetism in the actinide 115 superconductors, combined with the observed Curie paramagnetism, led us to recently propose [12] that the actinide 115s are composite pair superconductors [13], where the heavy Cooper pair forms by combining two electrons in two orthogonal Kondo channels with a spin flip to form a composite pair, $\Lambda_C = \langle N + 2|c^\dagger_{1\downarrow} c^\dagger_{2\downarrow} S_+|N\rangle$, where $c^\dagger_{1,2}$ create electrons in two orthogonal Kondo screening channels [12,14].

This presents us with a dichotomy, for while composite pairing may account for the quenching of local moments at the transition temperature, it fails to account for the importance of magnetism in the Ce 115 phase diagram. To resolve this issue, here we propose that magnetic and composite pairing work in tandem to drive superconductivity. Composite pairing originates from two-channel Kondo impurities, while magnetic pairing emerges from antiferromagnetically coupled Kondo impurities. Observing that these two systems are equivalent at criticality in the dilute limit [15], here we argue that this connection persists to the lattice superconducting state concealing a common quantum critical point (QCP) [16].

To expose the interplay between magnetic and composite pairing, we examine the internal structure of a heavy-fermion pair. In a Kondo lattice, the heavy quasiparticles are a linear combination $a^\dagger_{\mathbf{k}\uparrow} = u_\mathbf{k} c^\dagger_{\mathbf{k}\uparrow} + v_\mathbf{k} f^\dagger_{\mathbf{k}\uparrow}$, where $c^\dagger$ and $f^\dagger$ create conduction and localized electrons, respectively [17]. The wave function is

$$|\Psi\rangle = P_G \exp(\Lambda^\dagger)|0\rangle, \tag{1}$$

where $\Lambda^\dagger = \sum_\mathbf{k} \Delta_k (a^\dagger_{\mathbf{k}\uparrow} a^\dagger_{-\mathbf{k}\downarrow})$ creates a d-wave pair of quasiparticles and P_G is the Gutzwiller projection operator restricting the number of f electrons to one. Acting the Gutzwiller projector on the f electron reveals its internal structure as a composite between a conduction electron and a spin flip at a given site j, $P_G f^\dagger_{j\sigma} \sim c^\dagger_{j\tau}(\vec{\sigma} \cdot \vec{S}_j)_{\tau\sigma} P_G$. The pairing field $\Lambda^\dagger$ contains three terms

$$\Lambda^\dagger = \sum_\mathbf{k} \begin{pmatrix} c^\dagger_{\mathbf{k}\uparrow}, & f^\dagger_{\mathbf{k}\uparrow} \end{pmatrix} \begin{bmatrix} \Delta^e_\mathbf{k} & \Delta^C_\mathbf{k} \\ \Delta^C_\mathbf{k} & \Delta^M_\mathbf{k} \end{bmatrix} \begin{pmatrix} c^\dagger_{-\mathbf{k}\downarrow} \\ f^\dagger_{-\mathbf{k}\downarrow} \end{pmatrix} = \Psi^\dagger_e + \Psi^\dagger_C + \Psi^\dagger_M. \tag{2}$$

The diagonal terms, with $\Delta^e_\mathbf{k} = u^2_\mathbf{k} \Delta_\mathbf{k}$ and $\Delta^M_\mathbf{k} = v^2_\mathbf{k} \Delta_\mathbf{k}$ create f- and conduction electron pairs, where a d-wave pair of f electrons is an intersite operator, taking the form

$$\Psi^\dagger_M = \sum_{i,j} \Delta^M(\mathbf{R}_{ij})[c^\dagger_i (\vec{\sigma} \cdot \vec{S}_j)(i\sigma_2)(\vec{\sigma}^T \cdot \vec{S}_j) c^\dagger_j] \tag{3}$$

outside the Gutzwiller projection. However, if we expand the off-diagonal terms in real space,

$$\Psi^\dagger_C = \sum_{i,j} \Delta^C(\mathbf{R}_{ij})[c^\dagger_i (i\sigma_2)(\vec{\sigma}^T \cdot \vec{S}_j) c^\dagger_j] \tag{4}$$

where $\Delta^C(\mathbf{R}) = \sum_\mathbf{k} (u_\mathbf{k} v_\mathbf{k} \Delta_\mathbf{k}) e^{i\mathbf{k}\cdot\mathbf{R}}$, we find a composite pair formed between a triplet pair of conduction electrons and a spin flip [12–14]. Unlike its diagonal counterparts, which are necessarily intersite, composite pairs are

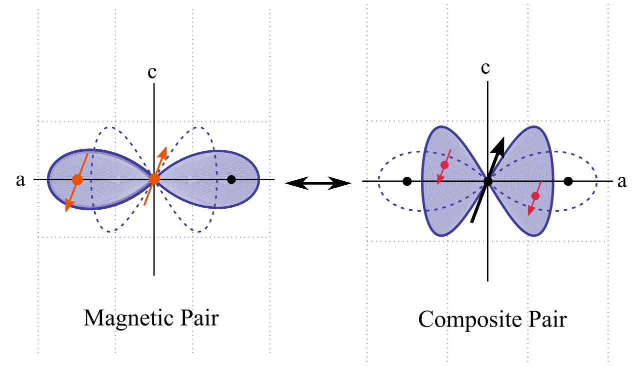

FIG. 1 (color online). A tandem pair contains a superposition of magnetic and composite pairing, both with d-wave symmetry. The magnetic pair (left) contains neighboring f electrons, while the composite pair (right) combines a spin flip and two conduction electrons. The unit cell is denoted by dotted lines, with dots indicating the local moment sites.

compact objects formed from pairs of orthogonal Wannier states surrounding a single local moment (Fig. 1).

Magnetic interactions favor the intersite component of the pairing, while the two-channel Kondo effect favors the composite intrasite component. However, both components will always be present in the superconducting Kondo lattice. If the composite and magnetic order parameters share a d-wave symmetry, they will necessarily couple linearly to one another, as we shall show next. This coupling enhances the transition temperature over a large region of the phase diagram, providing a natural explanation for both the actinide and Ce 115 compounds.

To illustrate tandem pairing microscopically, we introduce the two-channel Kondo-Heisenberg model,

$$H = H_c + H_{K1} + H_{K2} + H_M \tag{5}$$

and solve it exactly in the symplectic large-N limit [12], where

$$H_c = \sum_{\mathbf{k}} \epsilon_{\mathbf{k}} c^\dagger_{\mathbf{k}\sigma} c_{\mathbf{k}\sigma}, \qquad H_M = J_H \sum_{\langle ij \rangle} \vec{S}_i \cdot \vec{S}_j, \tag{6}$$

$$H_{K\Gamma} = J_\Gamma \sum_j \psi^\dagger_{j\Gamma a} \vec{\sigma}_{ab} \psi_{j\Gamma b} \cdot \vec{S}_j. \tag{7}$$

Here $\vec{S}_j$ is the local moment on site j, and $\psi_{j\Gamma}$ is the Wannier state representing a conduction electron on site j with symmetry Γ,

$$\psi_{j\Gamma a} = \sum_{\mathbf{k}} \Phi_{\Gamma \mathbf{k} ab} c_{\mathbf{k} b} e^{i\mathbf{k}\cdot\mathbf{R}_j}, \tag{8}$$

where the form factor $\Phi_{\Gamma kab}$ is only diagonal in the spin indices in the absence of spin orbit. Microscopically, the two orthogonal Kondo channels J_Γ arise from virtual fluctuations from the ground state doublet to excited singlets, where the two channels correspond to adding and removing an electron, respectively. In Ce, the $4f^1$ state is split by tetragonal symmetry into three Kramer's doublets, where Γ_7^+ is the ground state doublet [18,19], so we may summarize the virtual valence fluctuations with

$$4f^0(\cdot) \overset{\Gamma_7^+}{\rightleftharpoons} 4f^1(\Gamma_7^+) \overset{\Gamma_6}{\rightleftharpoons} 4f^2(\Gamma_7^+ \otimes \Gamma_6). \tag{9}$$

Requiring the composite pairing to resonate with the d-wave magnetic pairing [20] uniquely selects $\Gamma_7^+ \otimes \Gamma_6$ as the lowest doubly occupied state, as this combination leads to d-wave composite pairing [12]. A simplified two-dimensional model is sufficient to illustrate the basic physics, where the d-wave composite pair now comes from the combination of s-wave hybridization in channel one and d-wave hybridization in channel two [21,22]. The magnetism is included as an explicit RKKY interaction, J_H between neighboring local moments $\langle ij \rangle$, generated by integrating out electron in bands far from the Fermi surface. Treating the magnetism as a Heisenberg term leads to a two band version of resonating valence bond (RVB) superconductivity [23], where the local moments form valence bonds which can "escape" into the conduction sea through the Kondo hybridization to form charged, mobile Cooper pairs [24,25].

To solve this model, we use the fermionic symplectic spin representation, $S_{\alpha\beta}(j) = f^\dagger_{j\alpha} f_{j\beta} - \mathrm{sgn}(\alpha\beta) f^\dagger_{j-\beta} f_{j-\alpha}$, where $\alpha \in \{-N/2, \ldots, N/2\}$. This symplectic-$N$ representation maintains the time-reversal properties of SU(2) for all even N, enabling the consistent treatment of superconductivity [12]. The spin Hamiltonians become

$$H_{K\Gamma}(j) = -\frac{J_\Gamma}{N}[(\psi^\dagger_{j\Gamma} f_j)(f^\dagger_j \psi_{j\Gamma}) + (\psi^\dagger_{j\Gamma} \epsilon^\dagger f^*_j)(f^T_j \epsilon \psi_{j\Gamma})],$$
$$H_M(ij) = -\frac{J_H}{N}[(f^\dagger_i f_j)(f^\dagger_j f_i) + (f^\dagger_i \epsilon^\dagger f^*_j)(f^T_j \epsilon f_i)], \tag{10}$$

where we have suppressed the spin indices by treating them as vectors of length N; ϵ is the large N generalization of $i\sigma_2$, and $f^*_j = (f^\dagger)^T$. Each quartic term can be decoupled by a Hubbard-Stratonovich field, leading to normal, $V_\Gamma \propto \langle c^\dagger_\Gamma f \rangle$, and anomalous, $\Delta_\Gamma \propto \langle c^\dagger_\Gamma \epsilon f^\dagger \rangle$, hybridization in each Kondo channel, and particle-hole, $h_{ij} \propto \langle f^\dagger_i f_j \rangle$, and pairing, $\Delta^H_{ij} \propto \langle f^\dagger_i \epsilon f^\dagger_j \rangle$, terms for the spin liquid, where $\langle \cdots \rangle$ represents a thermal expectation value. This Hamiltonian possesses an SU(2) gauge symmetry, $f \to uf + v\epsilon^\dagger f^\dagger$, which we use to eliminate Δ_1, and composite pair superconductivity occurs when $V_1 \Delta_2 \sim \langle c^\dagger_1 c^\dagger_2 \epsilon f^\dagger f \rangle$ is nonzero [12]. We calculate the mean-field values of these fields using the saddle point approximation, which becomes exact as $N \to \infty$. The lowest energy solutions involve only pairing fields in the magnetic and second Kondo channels, giving rise to only three nonzero Hubbard-Stratonovich fields, V_1, Δ_2, and Δ_H [26]. We take Δ_H to be d wave in the plane, so that $\Delta^H_k \equiv \Delta_H(\cos k_x - \cos k_y)$; in this simple model, $\Phi_1 = 1$ and $\Phi_2 = (\cos k_x - \cos k_y)$. Using the Nambu notation, $\tilde{c}^\dagger_{\mathbf{k}} = (c^\dagger_{\mathbf{k}}, \epsilon c_{-\mathbf{k}})$, $\tilde{f}^\dagger_{\mathbf{k}} = (f^\dagger_{\mathbf{k}}, \epsilon f_{-\mathbf{k}})$, and defining the matrix $\mathcal{V}_k = V_1 \Phi_{1\mathbf{k}} \tau_3 + \Delta_2 \Phi_{2\mathbf{k}} \tau_1$, the mean-field Hamiltonian can be concisely written as

$$H = \sum_k (\tilde{c}_k^\dagger \quad \tilde{f}_k^\dagger) \begin{bmatrix} \epsilon_k \tau_3 & \mathcal{V}_k^\dagger \\ \mathcal{V}_k & \lambda\tau_3 + \Delta_{Hk}\tau_1 \end{bmatrix} \begin{pmatrix} \tilde{c}_k \\ \tilde{f}_k \end{pmatrix} + N\left(\frac{V_1^\dagger V_1}{J_1} + \frac{\Delta_2^\dagger \Delta_2}{J_2} + \frac{4\Delta_H^2}{J_H}\right), \quad (11)$$

where λ is the Lagrange multiplier enforcing the constraint $n_f = N/2$. The mean-field Hamiltonian can be diagonalized analytically. Upon minimizing the free energy, we obtain four equations for λ, V_1, Δ_2, and Δ_H. Solving these numerically, and searching the full parameter space of J_2/J_1, J_H/J_1, and T to find both first and second order phase transitions, we find four distinct phases: a light Fermi liquid with free local moments when all parameters are zero, at high temperatures; a heavy Fermi liquid when either V_1 or Δ_2 are finite, with symmetry Γ, below $T_{K\Gamma}$; a spin liquid state decoupled from a light Fermi liquid when Δ_H is finite, below $T_{\rm SL}$; and a tandem superconducting ground state with V_1, Δ_2 and Δ_H all finite, below T_c, as shown in Fig. 2. There is no long range magnetic order due to our fermionic spin representation. The superconductivity is stable with respect to the massive $1/N$ gauge fluctuations, however, it is an interesting open question whether the resulting quasiparticle renormalizations will generate a spin resonance mode.

Experimentally, CeMIn$_5$ can be continuously tuned from M = Co to Rh to Ir [3]. While CeRhIn$_5$ is a canonical example of a magnetically paired superconductor, where moderate pressure reveals a superconducting dome as the Néel temperature vanishes [1], further pressure [27] or Ir doping on the Rh site [3] leads to a second dome, where spin fluctuations are weaker [28]. We assume that the changing chemical pressure varies the relative strengths of the Kondo and RKKY couplings, so that doping traces out a path through the phase diagram like the one in Fig. 3, chosen for its similarities to CeMIn$_5$. By maintaining the same Fermi liquid symmetry throughout ($T_{K1} > T_{K2}$), we are restricted to one (mostly magnetic) or two (magnetic and tandem) domes.

A qualitative understanding of this tandem pairing can be obtained within a simple Landau expansion. For $T \sim T_c \ll T_{K1}$, $\Phi \equiv \Delta_2$ and $\Psi \equiv \Delta_H$ will be small, and the free energy can be expressed as

$$F = \alpha_1(T_{c1} - T)\Psi^2 + \alpha_2(T_{c2} - T)\Phi^2 + 2\gamma\Psi\Phi + \beta_1\Psi^4 + \beta_2\Phi^4 + 2\beta_i\Psi^2\Phi^2, \quad (12)$$

$\alpha_{1,2}$, $\beta_{1,2,i}$, and γ are all functions of λ and V_1 and can be calculated exactly in the mean-field limit. The linear coupling of the two order parameters, $\gamma = \partial^2 F/\partial\Delta_2\partial\Delta_H$, is always nonzero in the heavy Fermi liquid because the hybridization, V_1 converts one to the other, $f^\dagger f^\dagger \sim V_1 c^\dagger f^\dagger$. The linear coupling enhances the transition temperature,

$$T_c = \frac{T_{c1} + T_{c2}}{2} + \sqrt{\left(\frac{T_{c1} - T_{c2}}{2}\right)^2 + \frac{\gamma^2}{\alpha_1\alpha_2}}. \quad (13)$$

For $\beta_1\beta_2 > \beta_i^2$, the two order parameters are only weakly repulsive, leading to smooth crossovers from magnetic to composite pairing under the superconducting dome [29].

While the development of conventional superconductivity does not change the underlying charge distribution, tandem pairing is electrostatically active, as composite pairing redistributes charge, leading to an electric quadrupole moment. The transition temperature of the 115 superconductors is known to increase linearly with the lattice

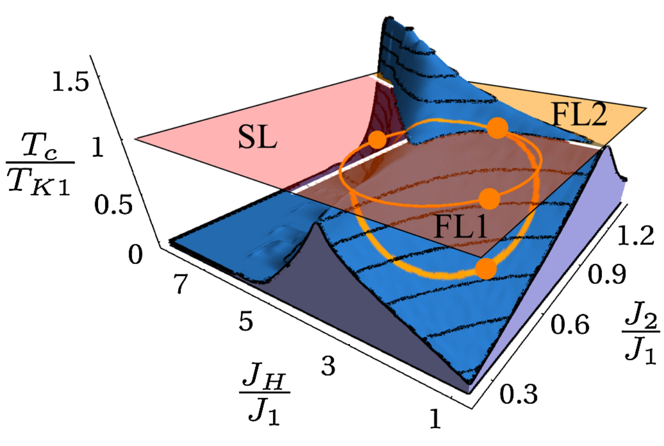

FIG. 2 (color online). The superconducting transition temperature as the amounts of magnetic, J_H, and second channel, J_2, couplings are varied ($\Phi_1 = 1$, $\Phi_2 = \cos k_x - \cos k_y$, and $n_c = 0.75$). V_1, Δ_2, and Δ_H are all nonzero everywhere below T_c. A slice at $T = T_{K1}$ shows the regions of the spin liquid and Fermi liquids, and the orange ellipse illustrates how materials could tune the relative coupling strengths (see Fig. 3). The transition is first order for $J_H/J_1 > 4$.

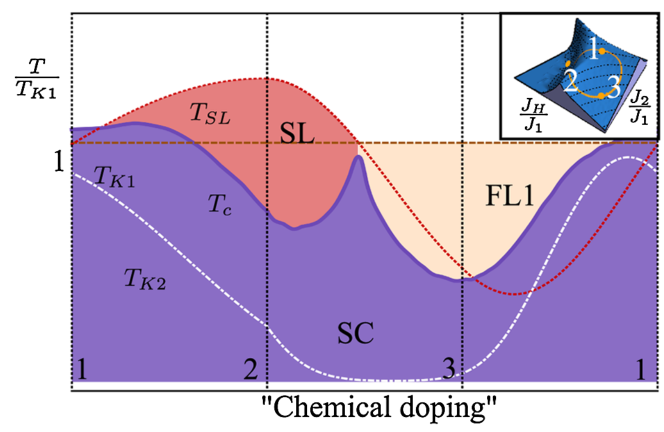

FIG. 3 (color online). A possible experimental path through the phase diagram in Fig. 2, chosen for its similarity to the Ce 115 doping phase diagram [3], described by the orange ellipse, $(\frac{J_2/J_1 - 0.4}{0.2})^2 + (\frac{J_H/J_1 - 0.9}{0.16})^2 = 1$. The transition temperatures for superconductivity, T_c (solid blue), spin liquid, $T_{\rm SL}$ (dotted red), and Fermi liquids, T_{K1} (dashed orange) and T_{K2}, (dot-dashed white) are also plotted. All temperatures are scaled by T_{K1}. While our ground state is always superconducting, due to the fermionic spin representation, real materials will be antiferromagnetic for $T_{\rm SL} \gg T_{K1}$.

c/a ratio [30], conventionally attributed to decreasing dimensionality. Our theory suggests an alternative interpretation: as the condensate quadrupole moment, $Q_{zz} \propto \Psi_C^2$ couples linearly to the tetragonal strain, $\Delta F \propto -Q_{zz}u_{\rm tet}$, the second term in the Landau free energy (12) becomes $\alpha_2[T - (T_{c2} + \lambda u_{\rm tet})]\Psi_C^2$, naturally accounting for the linear increase in T_c. This effect should also be detectable as a shift of the nuclear quadrupole resonance (NQR) frequency at the surrounding nuclei.

The link between f-electron valence and the Kondo effect is well established [31], but tandem pairing introduces a new element to this relationship. Changes in the charge distribution around the Kondo ion can be read off from its coupling to the changes in the chemical potential, $\Delta\rho(x) = |e|\delta H/\delta\mu(x)$. The sensitivity of the Kondo couplings to μ is obtained from a Schrieffer-Wolff transformation of a two-channel Anderson model, which gives $J_\Gamma^{-1} = \Delta E_\Gamma / V_{\Gamma,0}^2$. Here, $V_{\Gamma,0}$ are the bare hybridizations and ΔE_Γ are the charge excitation energies. With a shift in $\mu \rightarrow \mu + \delta\mu(x)$, $\delta J_\Gamma^{-1} = \pm|\Phi_\Gamma(x)|^2\delta\mu(x)/V_{\Gamma,0}^2$. The sign is positive for J_1 and negative for J_2 because they involve fluctuations to the empty and doubly occupied states, respectively: $f^0 \overset{\Gamma_1}{\rightleftharpoons} f^1 \overset{\Gamma_2}{\rightleftharpoons} f^2$. Differentiating (11) with respect to $\delta\mu(x)$, the change in $\rho(x)$ will be

$$\Delta\rho(x) = |e|\left[\left(\frac{V_1}{V_{1,0}}\right)^2|\Phi_1(x)|^2 - \left(\frac{\Delta_2}{V_{2,0}}\right)^2|\Phi_2(x)|^2\right]. \quad (14)$$

For equal channel strengths, the total charge is constant, and the f ion will develop equal hole densities in Γ_7^+ and electron densities in Γ_6, leading to a positive change in the electric field gradient, $\partial E_z/\partial z \propto (T_c - T) > 0$ at the in-plane In site that will appear as a shift in the NQR frequencies growing abruptly below T_c (see Fig. 4).

The f-electron valence should also contain a small superconducting shift, observable with core-level x-ray spectroscopy, obtained by integrating (14): $\Delta n_f(T) \propto \Psi_C^2 \propto (T_c - T)$, as $\Psi_C \propto \Delta_2$ when $J_1 > J_2$. While the development of Kondo screening leads to a gradual valence decrease through T_K, as it is a crossover scale, the development of superconductivity is a phase transition, leading to a sharp mean-field increase. Observation of sharp shifts at T_c in either the NQR frequency or the valence would constitute an unambiguous confirmation of the electrostatically active tandem condensate.

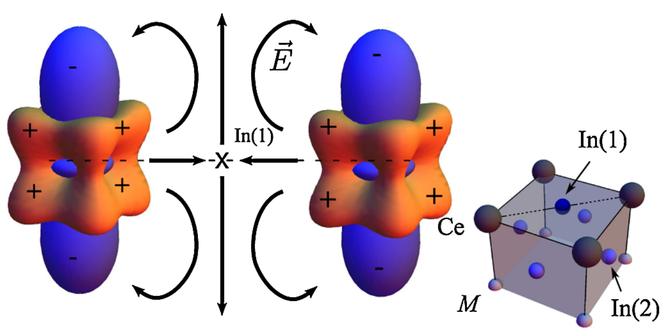

FIG. 4 (color online). As superconductivity develops, the increasing occupations of the empty and doubly occupied states cause holes to build up with symmetry Γ_7^+ (orange) and electrons with symmetry Γ_6 (blue). The resulting electric fields are shown along the [110] direction (dashed line in inset). The inset shows the locations of the indiums in-plane, In(1), and out-of-plane, In (2). The electric field gradient $\partial E_z/\partial z > 0$ at the In(1) site will lead to a sharp positive shift in the NQR frequency at T_c.

The authors would like to thank S. Burdin, C. Capan, Z. Fisk, H. Weber, R. Urbano, and particularly M. Dzero for discussions related to this work. This research was supported by National Science Foundation Grant No. DMR-0907179.

[1] H. Hegger *et al.*, Phys. Rev. Lett. **84**, 4986 (2000).
[2] C. Petrovic *et al.*, J. Phys. Condens. Matter **13**, L337 (2001).
[3] J. L. Sarrao and J. D. Thompson, J. Phys. Soc. Jpn. **76**, 051013 (2007).
[4] J. L. Sarrao *et al.*, Nature (London) **420**, 297 (2002).
[5] N. Mathur *et al.*, Nature (London) **394**, 39 (1998).
[6] K. Miyake, S. Schmitt-Rink, and C. M. Varma, Phys. Rev. B **34**, 6554 (1986).
[7] D. J. Scalapino, E. Loh, and J. E. Hirsch, Phys. Rev. B **34**, 8190 (1986).
[8] M. T. Béal-Monod, C. Bourbonnais, and V. J. Emery, Phys. Rev. B **34**, 7716 (1986).
[9] P. Monthoux and G. G. Lonzarich, Phys. Rev. B **66**, 224504 (2002).
[10] D. Aoki *et al.*, J. Phys. Soc. Jpn. **76**, 063701 (2007).
[11] H. Shishido *et al.*, J. Phys. Soc. Jpn. **71**, 162 (2002).
[12] R. Flint, M. Dzero, and P. Coleman, Nature Phys. **4**, 643 (2008).
[13] H. P. Dahal *et al.*, arXiv:0901.2323.
[14] P. Coleman, A. M. Tsvelik, N. Andrei, H. Y. Kee, Phys. Rev. B **60**, 3608 (1999).
[15] J. Gan, Phys. Rev. B **51**, 8287 (1995).
[16] D. L. Cox and M. Jarrell, J. Phys. Condens. Matter **8**, 9825 (1996).
[17] A. J. Millis and P. A. Lee, Phys. Rev. B **35**, 3394 (1987).
[18] A. D. Christianson *et al.*, Phys. Rev. B **70**, 134505 (2004).
[19] S. Nakatsuji *et al.*, Phys. Rev. Lett. **89**, 106402 (2002).
[20] W. K. Park, J. L. Sarrao, J. D. Thompson, and L. H. Greene Phys. Rev. Lett. **100**, 177001 (2008).
[21] P. Ghaemi and T. Senthil, Phys. Rev. B **75**, 144412 (2007).
[22] H. Weber and M. Vojta, Phys. Rev. B **77**, 125118 (2008).
[23] P. W. Anderson, Science **235**, 1196 (1987).
[24] N. Andrei and P. Coleman, Phys. Rev. Lett. **62**, 595 (1989).
[25] T. Senthil, S. Sachdev, and M. Vojta, Phys. Rev. Lett. **90**, 216403 (2003).
[26] A nonzero V_2 would indicate a composite nematic phase, which is unstable to superconductivity.
[27] T. Muramatsu *et al.*, J. Phys. Soc. Jpn. **70**, 3362 (2001).
[28] Shinji Kawasaki *et al.*, Phys. Rev. Lett. **94**, 037007 (2005); Phys. Rev. Lett. **96**, 147001 (2006).
[29] V. P. Mineev and M. E. Zhitomirsky, Phys. Rev. B **72**, 014432 (2005).
[30] E. D. Bauer *et al.*, Phys. Rev. Lett. **93**, 147005 (2004).
[31] O. Gunnarsson and K. Schonhammer, Phys. Rev. B **28**, 4315 (1983).